Electronic supplementary information (ESI) for:

L-Phenylalanine Monomer Coacervation Leads to Well-Controlled Nanocrystal Topochemical Photo-RAFT Polymerization

Yuting Li,[a] Xiyu Wang,[a] Ying Cao,[a] Wenjing Niu,[a] Qing Zheng,[a] Xinhua Lu[a] and Yuanli Cai*[a]

[a] *State-Local Joint Engineering Laboratory for Novel Functional Polymer Materials, Suzhou Key Laboratory of Macromolecular Design and Precision Synthesis, Jiangsu Engineering Laboratory of Novel Functional Polymeric Materials, Jiangsu Key Laboratory of Advanced Functional Polymer Materials, College of Chemistry, Chemical Engineering and Materials Science, Soochow University, Suzhou 215123, China*

Table S1. DLS Data (Light Scattering Intensity) of Reaction Coacervates of Topochemical Photo-RAFT Polymerization[a]

K1	**Conversion (%)**	**0**	**5**	**20**	**46**	**62**	**72**	**85**	**94**	**98**	**>99**
	Intensity (kcps)	0.5	0.5	0.5	0.6	0.6	0.6	0.6	0.7	0.7	0.7
K2	**Conversion (%)**	**0**	**2**	**18**	**37**	**57**	**74**	**83**	**92**	**97**	**>99**
	Intensity (kcps)	0.6	0.7	0.8	0.7	0.9	0.9	1.0	1.2	1.2	1.2

[a]Conditions: L-PheAm/CTCPA/SPTP = 50 (**K1**), 100 (**K2**), 25% w/w L-PheAm, water, pH 7.0, initially L-PheAm/CTCPA dispersion in water at pH 7.0 was stored at room temperature (~25 °C) overnight before starting the polymerization under visible light at 25 °C. Reaction dispersion was diluted to 5.0 mg/mL total solids content in Milli-Q water before DLS analysis.

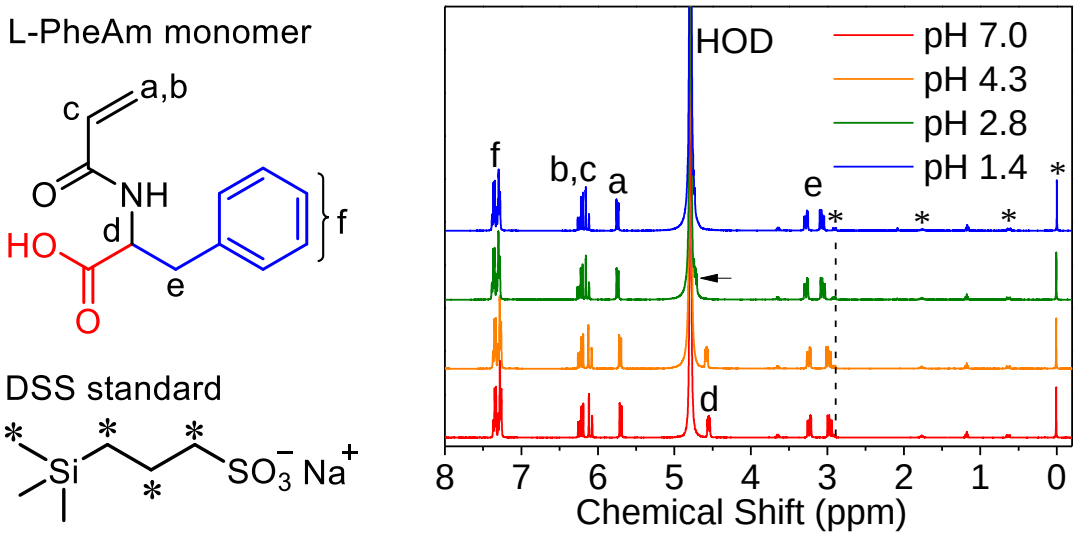

Fig. S1 ^{1}H NMR spectra of L-PheAm monomer at 4.0 mg/mL in D_2O at labelled pH values, in which DSS standard was used to determine the degree of solvation.

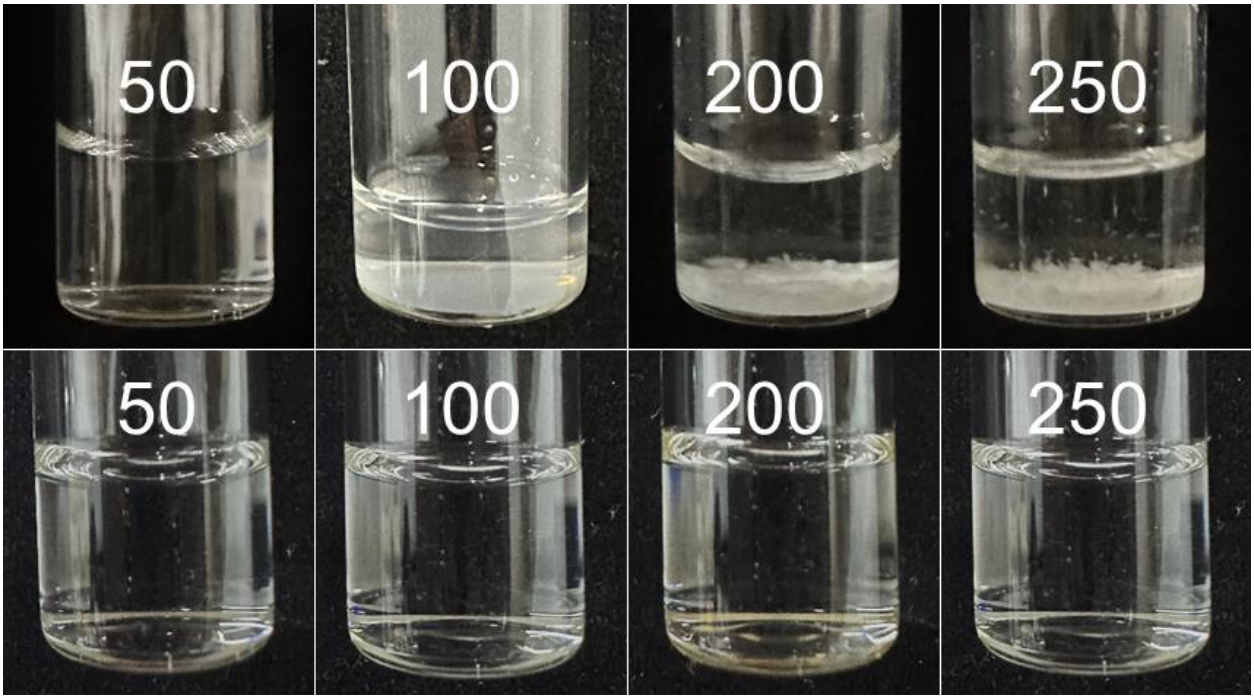

Fig. S2 Digital photographs of L-PheAm monomer dispersions at labelled concentrations (mg/mL) in water at pH 5.5 (top) and pH 7.0 (bottom).

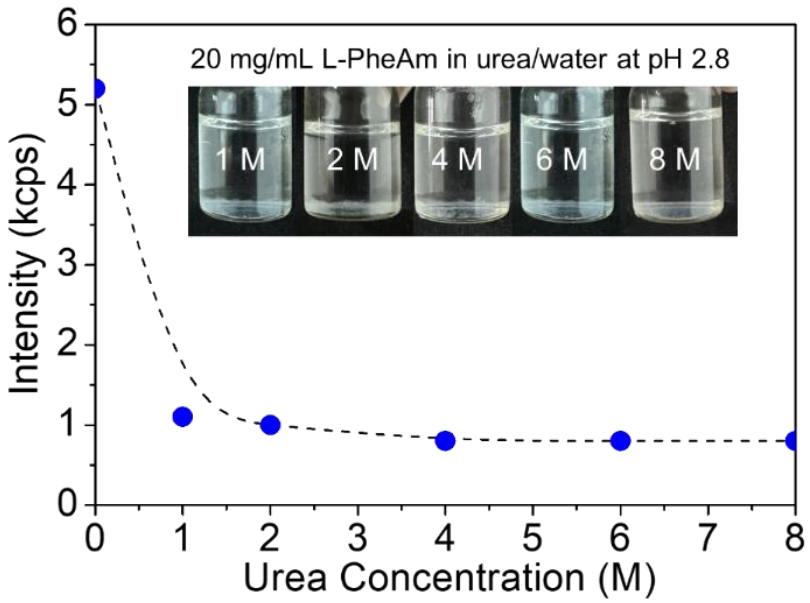

Fig. S3 Light scattering intensity versus the concentrations of urea added to 20.0 mg/mL L-PheAm monomer dispersion in water at pH 2.8. *Inset*: Digital photographs of the monomer/urea mixtures.

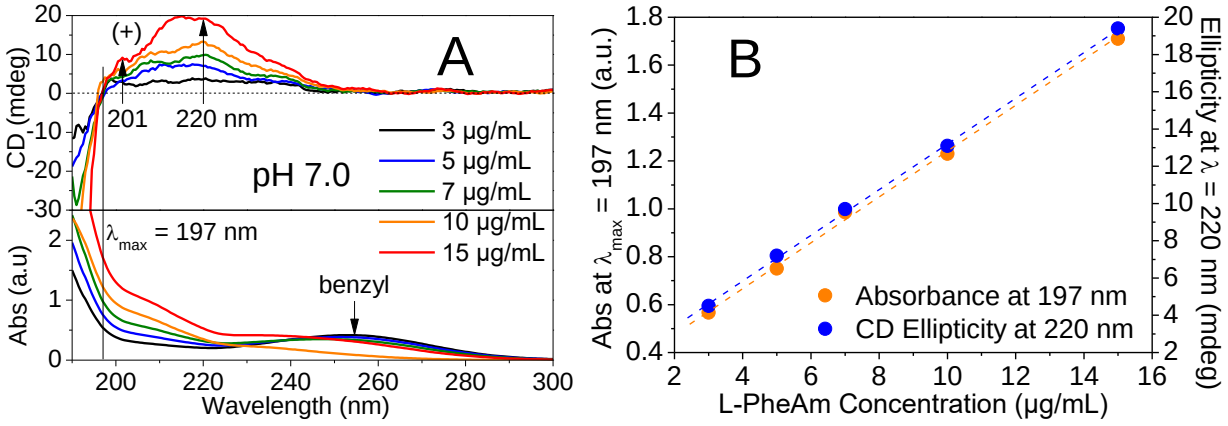

Fig. S4 Far-UV CD spectra of L-PheAm monomer at labelled concentrations in water at pH 7.0. (B) Monomer characteristic UV absorbance, CD bisignate band intensity versus concentrations.

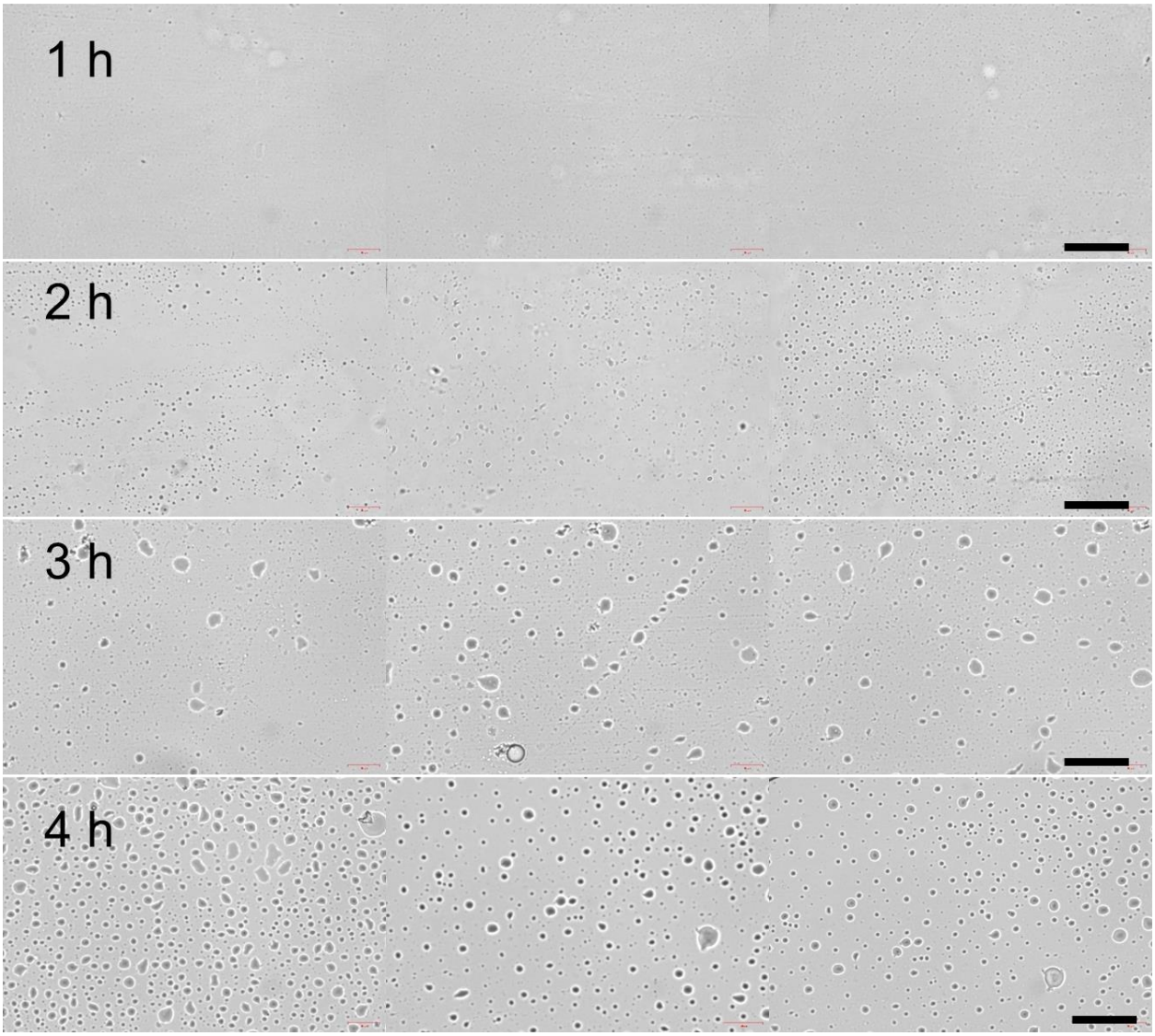

Fig. S5 Bright-field OM images showing Ostwald ripening upon neutralizing L-PheAm dispersion at 10.0 mg/mL in water at pH 10.5 to pH 7.0 at 25 °C, at labelled time points. Scale bar = 40 μm.

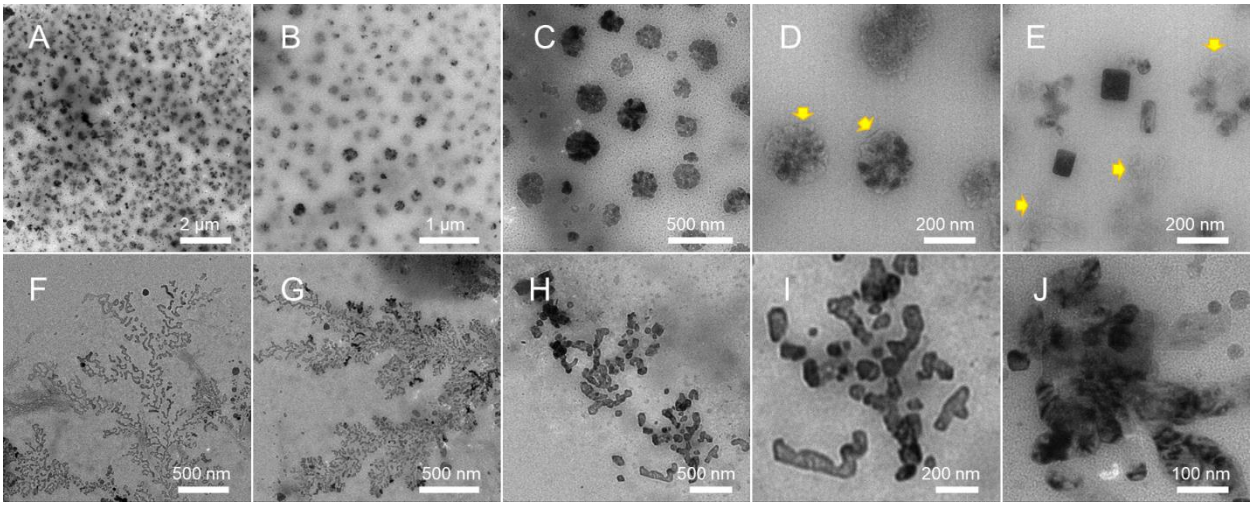

Fig. S6 Cryofixation TEM images showing transformation of (A-E) flower-shaped nanocrystal-containing coacervates (1 day, *arrow*: crystalline sheets) to (F-J) branched nanocrystal-containing coacervates incubated at 5 mg/mL L-PheAm in water at pH 5.5 for 20 days.

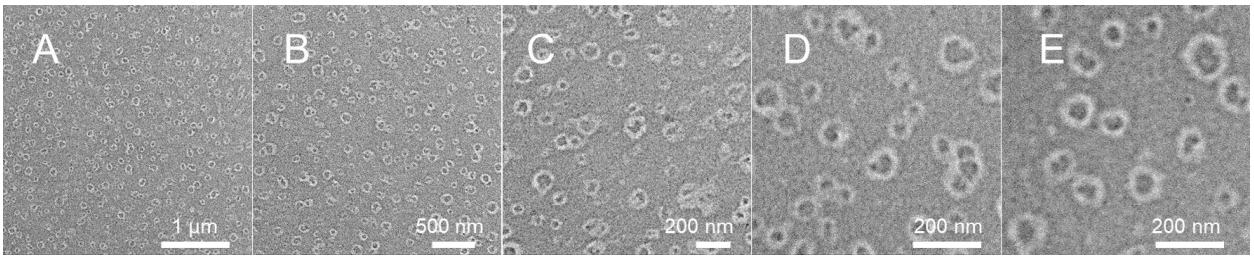

Fig. S7 Cryofixation TEM images of the nascent nanocrystals incubated at 0.2 mg/mL L-PheAm monomer in water at pH 7.0 for 20 days, where negligible liquid droplets indicates that the liquid-liquid phase separation (LLPS) was induced by the growing lamellar nanocrystals.

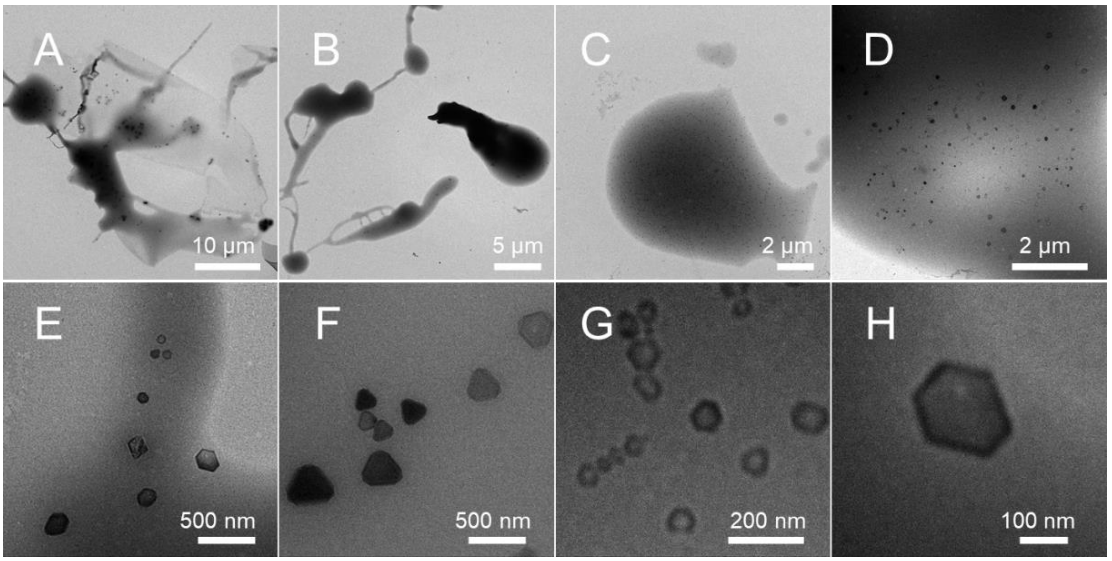

Fig. S8 Cryofixation TEM images showing (A-D) coacervates incubated at 5.0 mg/mL L-PheAm in water at pH 7.0 for 20 days; (E–H) higher magnificent TEM images showing discrete triangular and hexagonal nanocrystal lamellar sheets within the dense droplets.

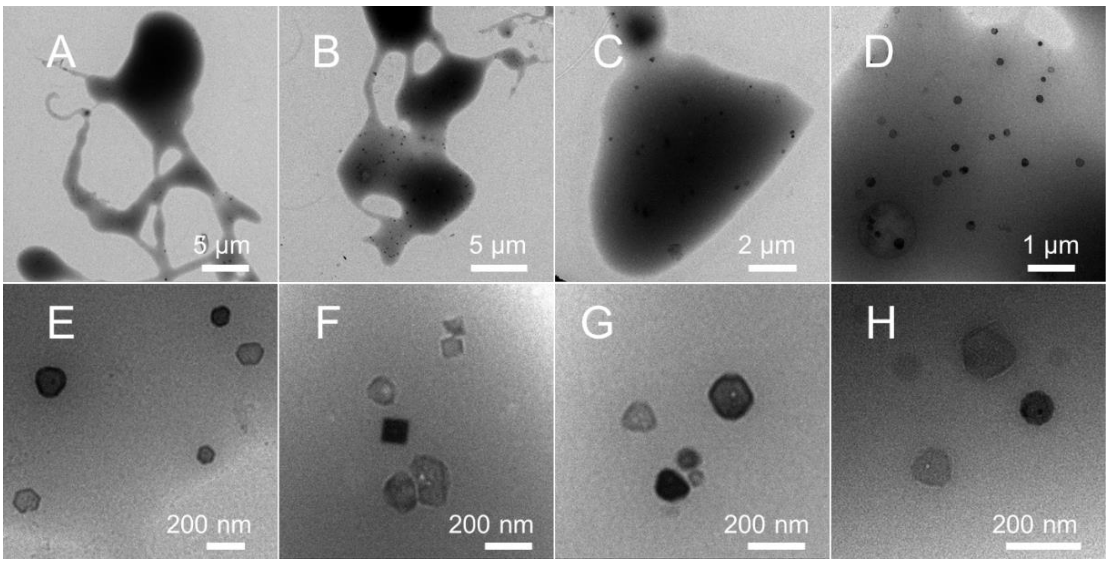

Fig. S9 Cryofixation TEM images showing (A–D) monomer self-coacervates upon dilution of the 20-d-incubated 5.0 mg/mL dispersion to 0.20 mg/mL in water, and further incubated overnight; (E–H) higher magnificent TEM images showing discrete nanocrystals within the dense droplets.

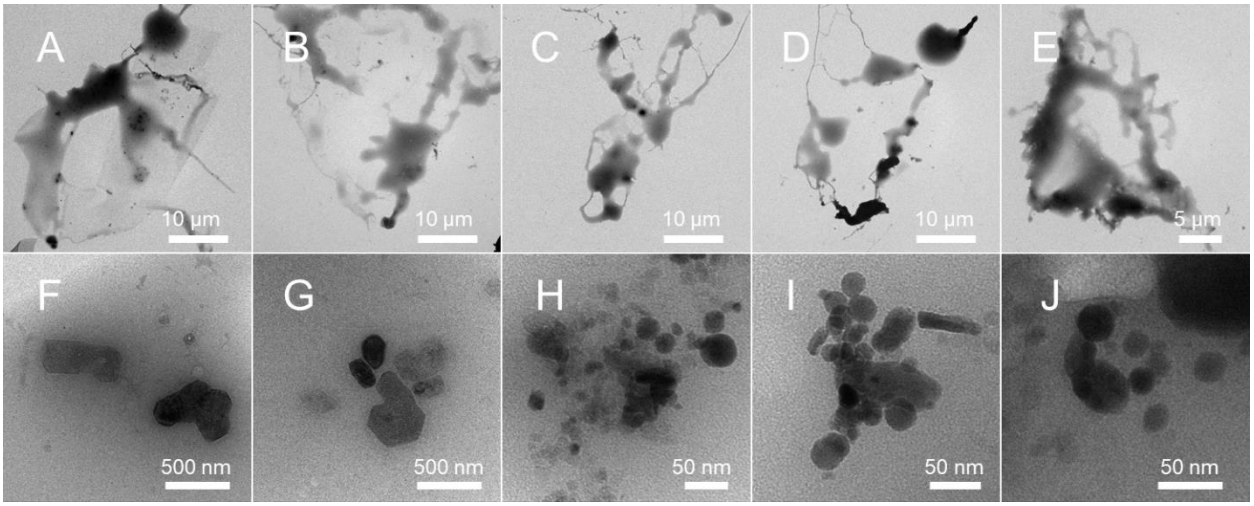

Fig. S10 (A–E) Cryofixation TEM images of CTCPA-doped monomer coacervates incubated at CTCPA/L-PheAm = 2/100 at 25% w/w L-PheAm in water at pH 7.0 overnight; (F-J) higher magnificent TEM images showing the interlinked nanocrystals within the dense droplets.

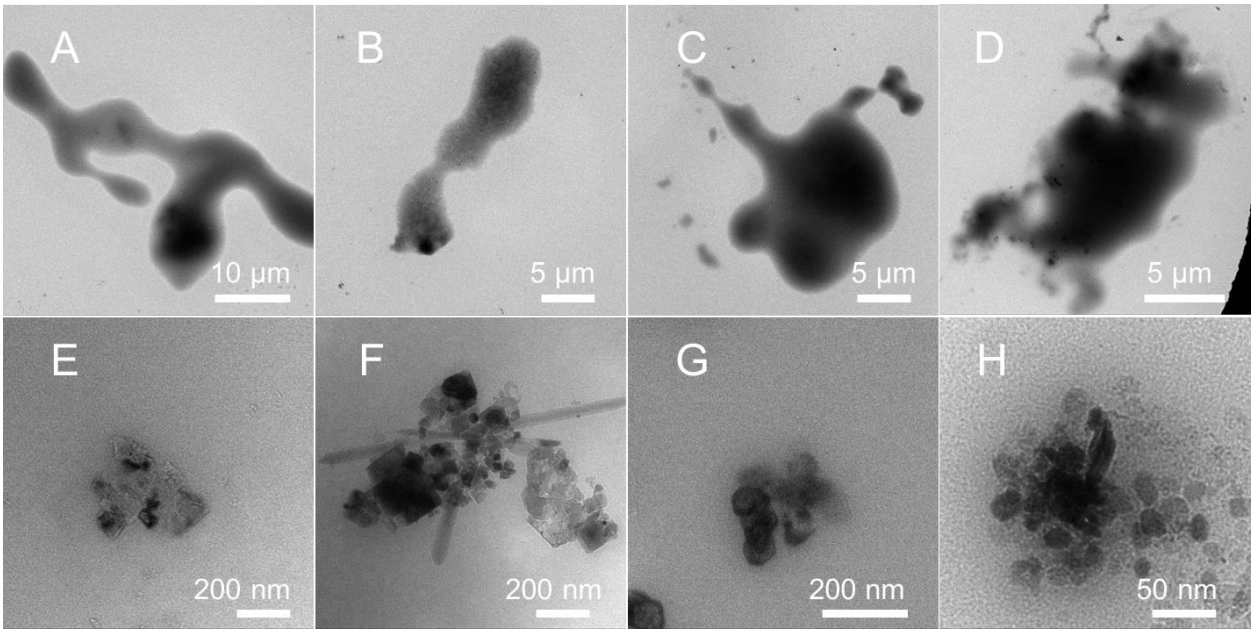

Fig. S11 (A–D) Cryofixation TEM images of CTCPA-doped monomer coacervates at CTCPA/L-PheAm = 1/100 at 25% w/w L-PheAm in water at pH 7.0 overnight; (E-H) higher magnificent TEM images showing the interlinked nanocrystals within the crowded droplets.

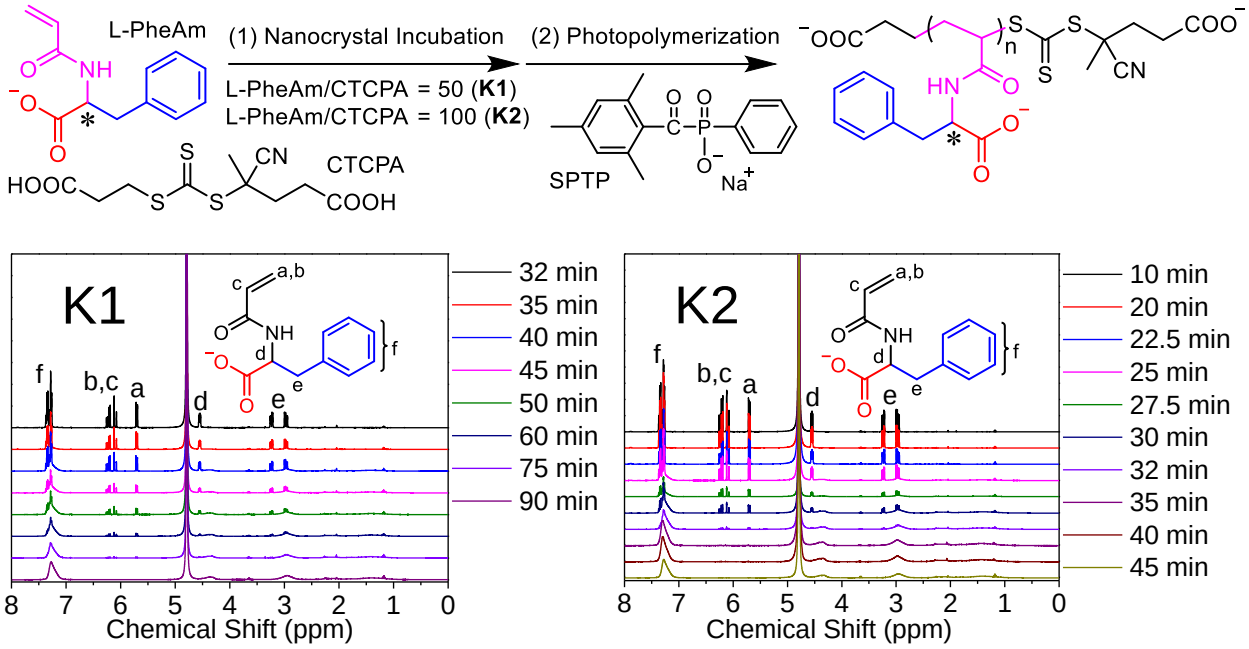

Fig. S12 ^{1}H NMR spectra of reaction dispersions at labelled time points of the topochemical photo-RAFT polymerization at L-PheAm/CTCPA/SPTP = 50:1:0.25 (**K1**) and 100:1:0.25 (**K2**) at 25% w/w L-PheAm in water at pH 7.0, under visible light at 25 °C. The CTCPA/L-PheAm dispersion was incubated at pH 7.0 overnight before starting photo-polymerization.

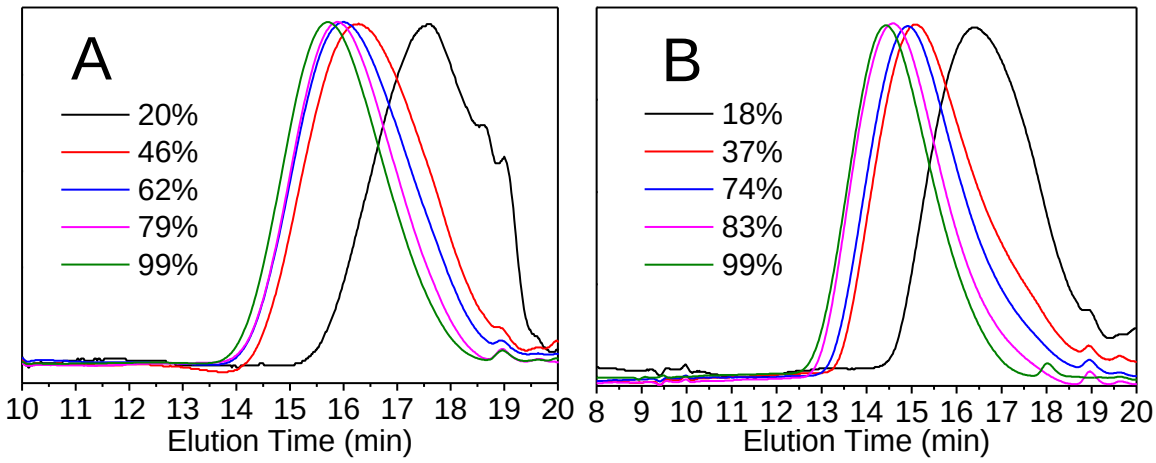

Fig. S13 Aqueous SEC traces of the polymers synthesized at labelled conversions of topochemical photo-RAFT polymerization. (A) **K1**, (B) **K2**.

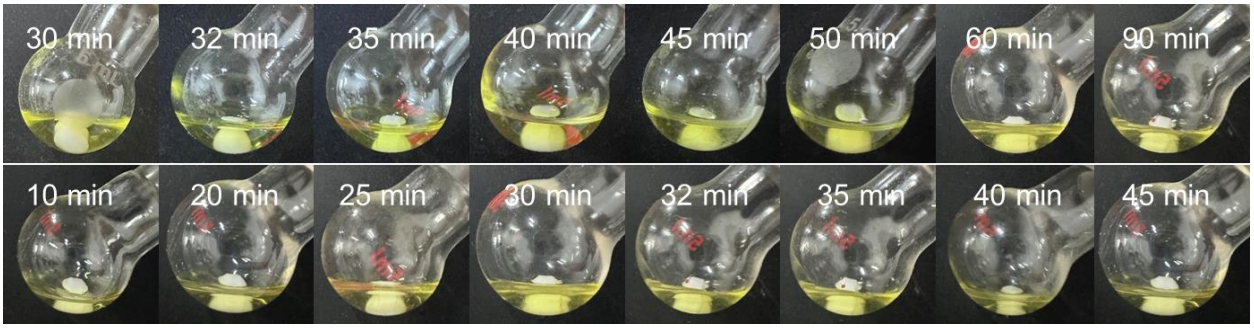

Fig. S14 Digital photographs of **K1** (top) and **K2** (bottom) dispersions at labelled time points.

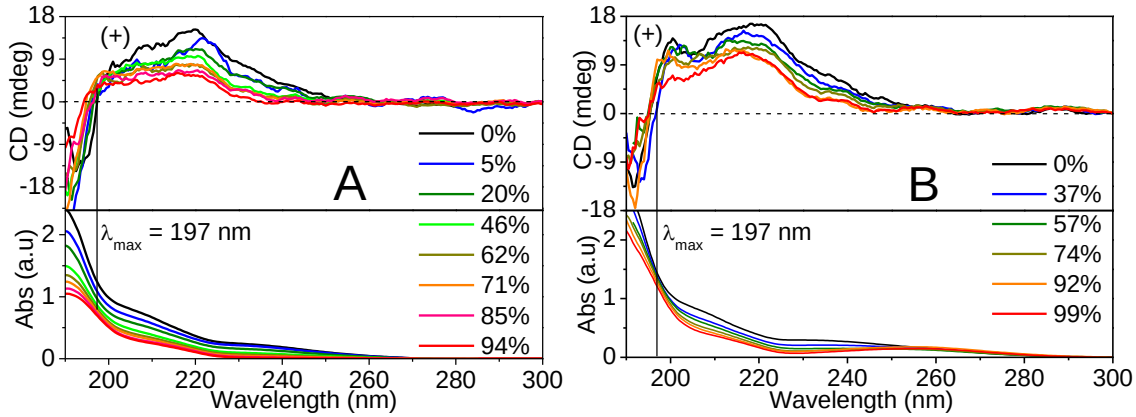

Fig. S15 Far-UV CD spectra of (A) **K1** and (B) **K2** reaction dispersions at labelled conversions.

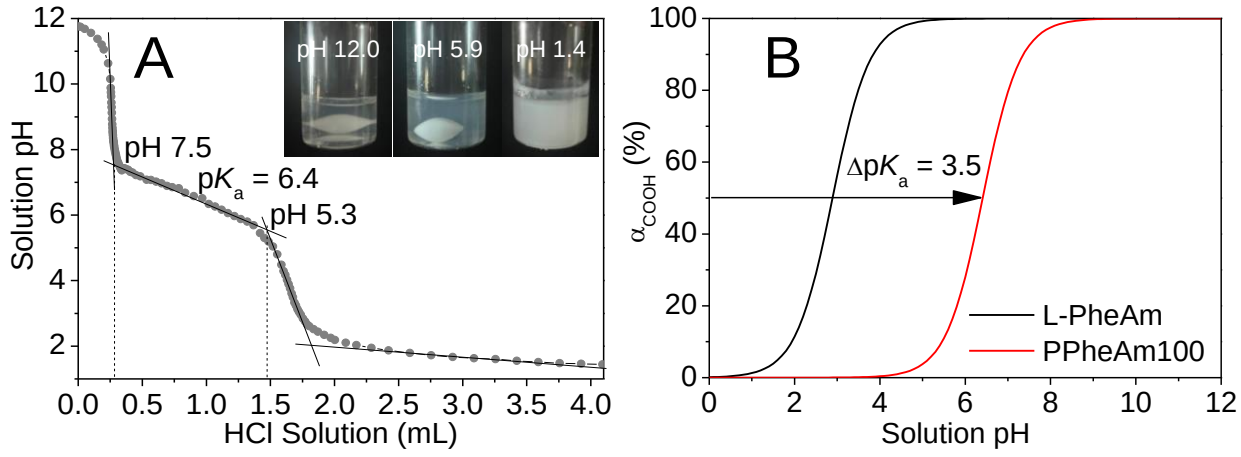

Fig. S16 (A) Potentiometric titration plots of PPheAm100 (11 mg/mL in water, 15 mL) titrated using 0.125 M HCl. (B) Degrees of ionization (α_{COOH}) versus solution pH values.

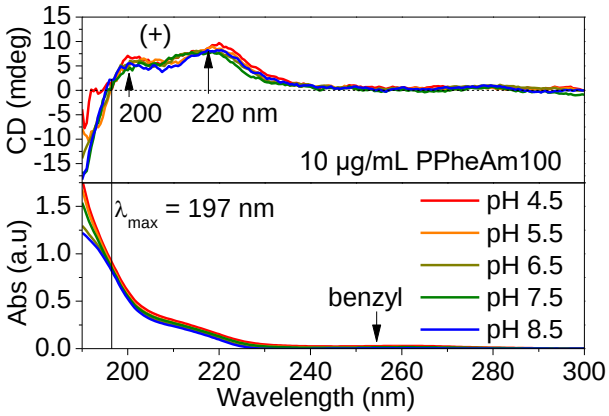

Fig. S17 Far-UV CD spectra of PPheAm100 (DP = 100) at 10 µg/mL at labelled pH. PPheAm100 was obtained by dialyzing and freeze-drying the **K2** final dispersion at >99% conversion.

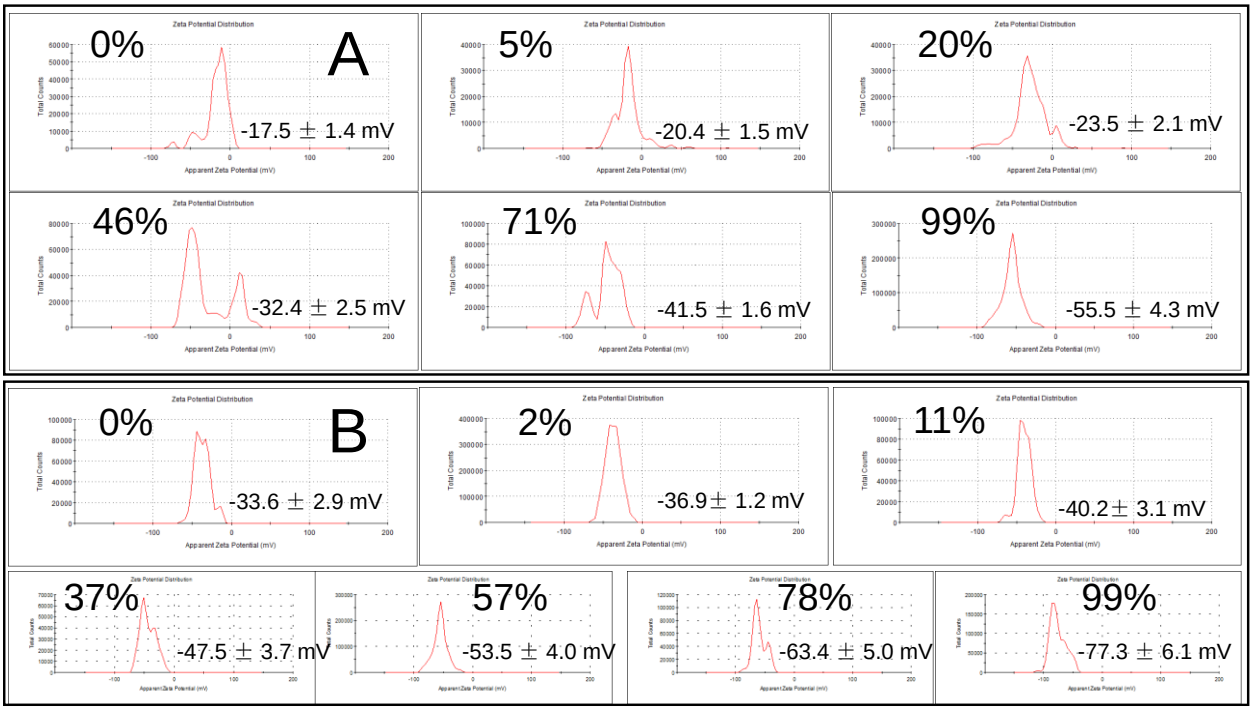

Fig. S18 Zeta potential (ζ) data of (A) **K1** and (B) **K2** reaction coacervates at labelled conversions. Each reaction dispersion was diluted to 5.0 mg/mL prior to zeta potential analysis.

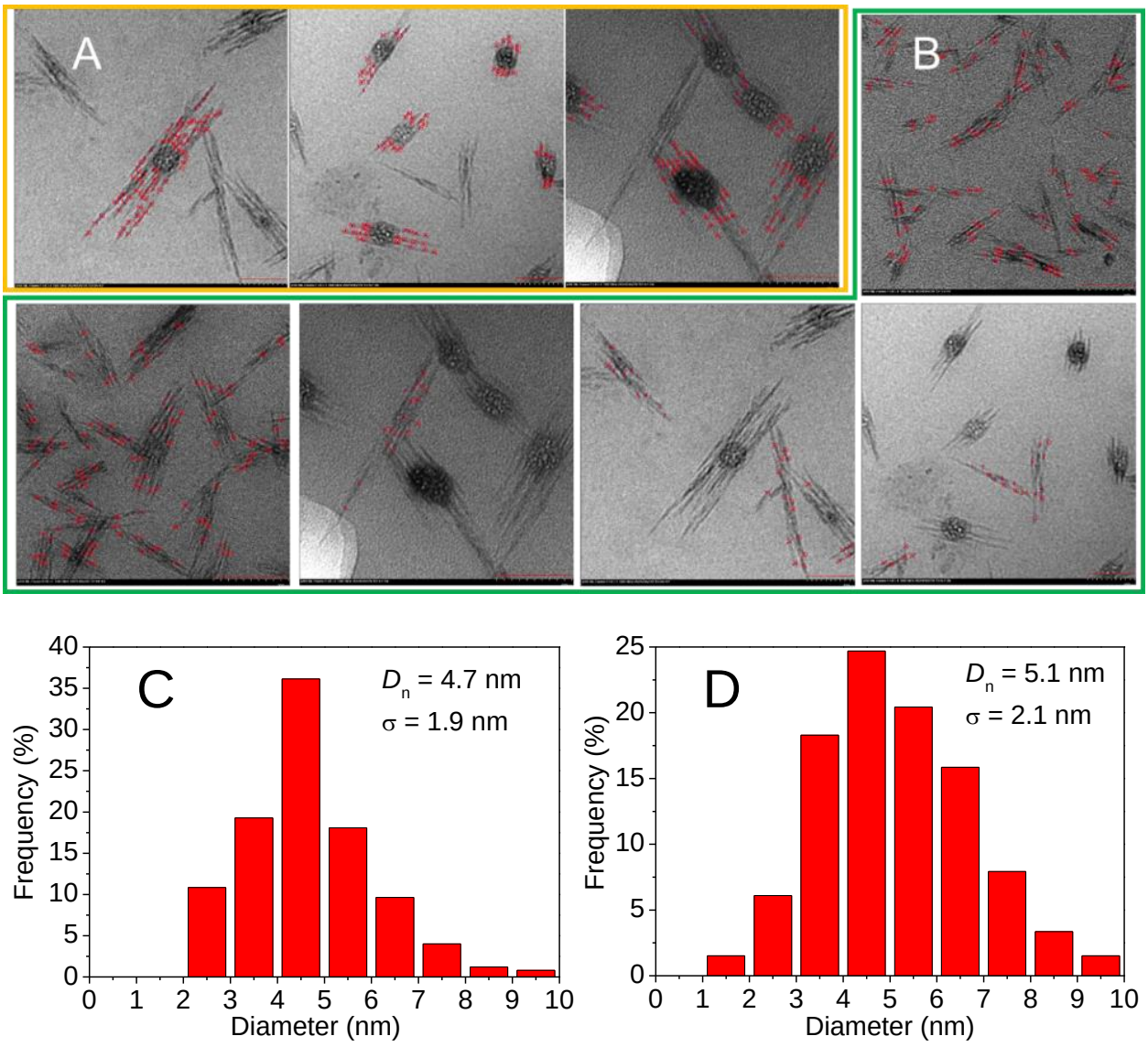

Fig. S19 TEM statistical data (D_n: mean diameter, σ: standard deviation) of (A) sieve-centered parallel-growing fibrils and (B) bundled fibrils within the **K1** coacervates at 20% conversion.

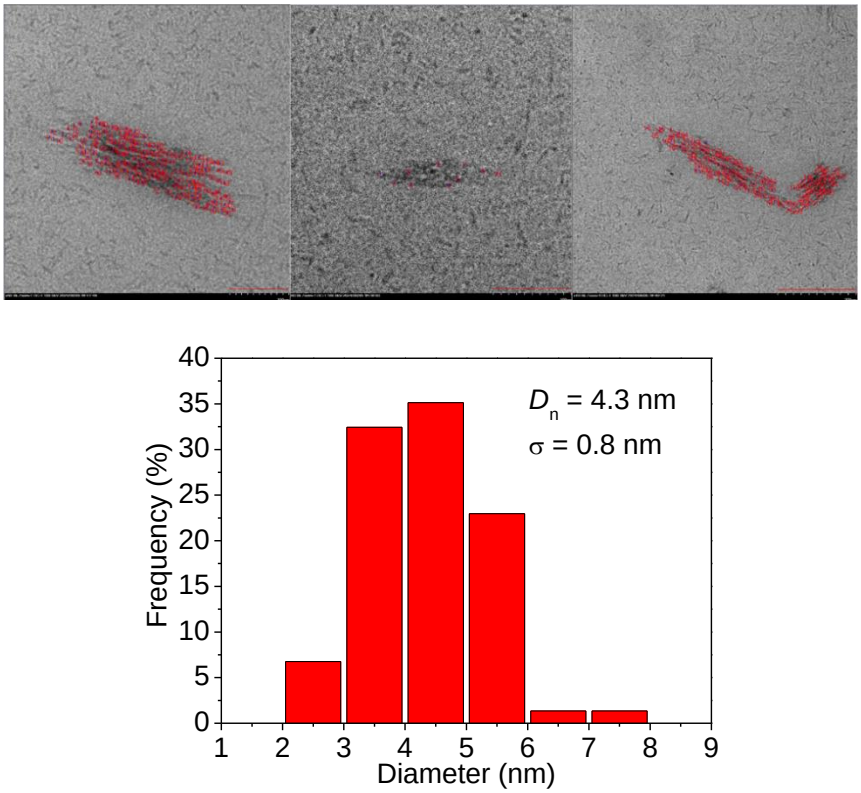

Fig. S20 TEM statistical analysis data (D_n: mean diameter, σ: standard deviation) of sieve-centered parallel fibrils and the bundled fibrils within the **K2** coacervates at 11% conversion.

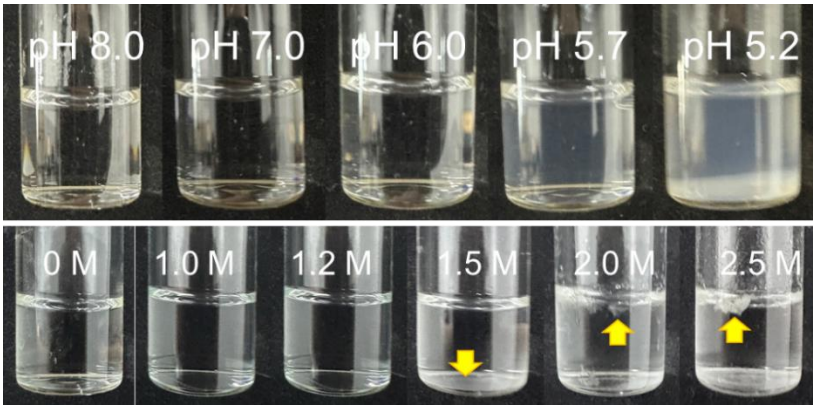

Fig. S21 Digital photographs of **K2** final dispersions upon (A) diluted to 5.0 mg/mL in pure water and adjusted to labeled pH values, (B) diluted to 5 mg/mL to pH 7.4 in salt water at labelled NaCl molar concentrations (*arrow*: salting-out floccules).

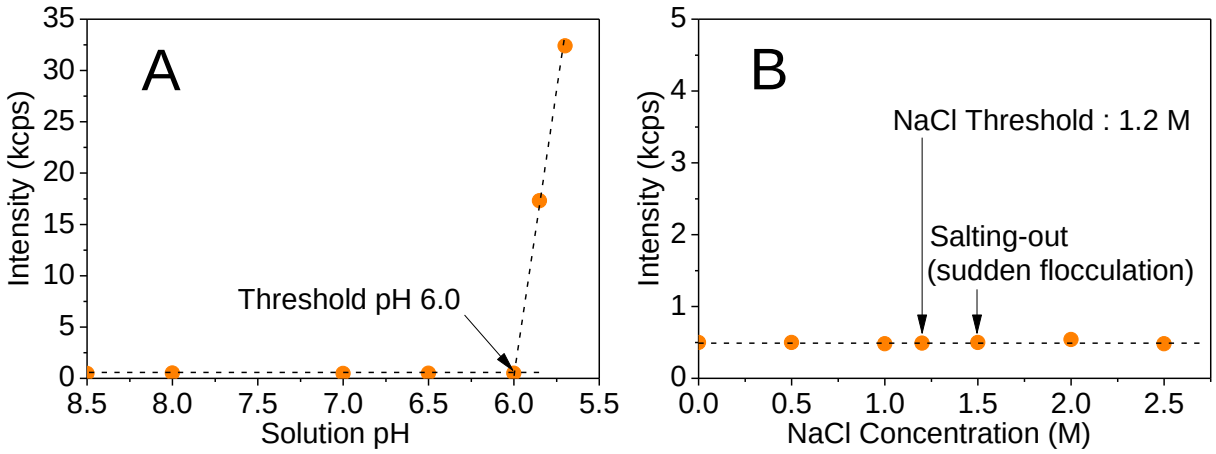

Fig. S22 Light scattering intensity versus (A) pH values of **K2** final dispersion upon diluted to 5.0 mg/mL in pure water, (B) NaCl concentrations of salt water used for diluting the dispersion to 5.0 mg/mL at pH 7.4.

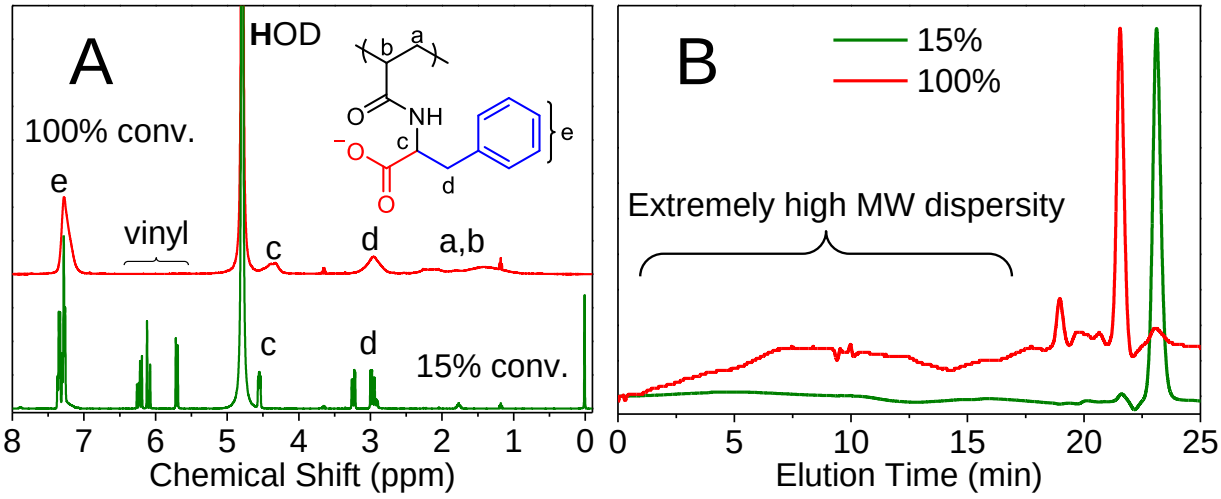

Fig. S23 (A) ^{1}H NMR spectra and (B) aqueous SEC traces of reaction dispersions of topochemical radical photopolymerization at L-PheAm/SPTP = 400:1 at 25% w/w L-PheAm in water at pH 7.0, under visible light at 25 °C for 5 min (green) and overnight (red).

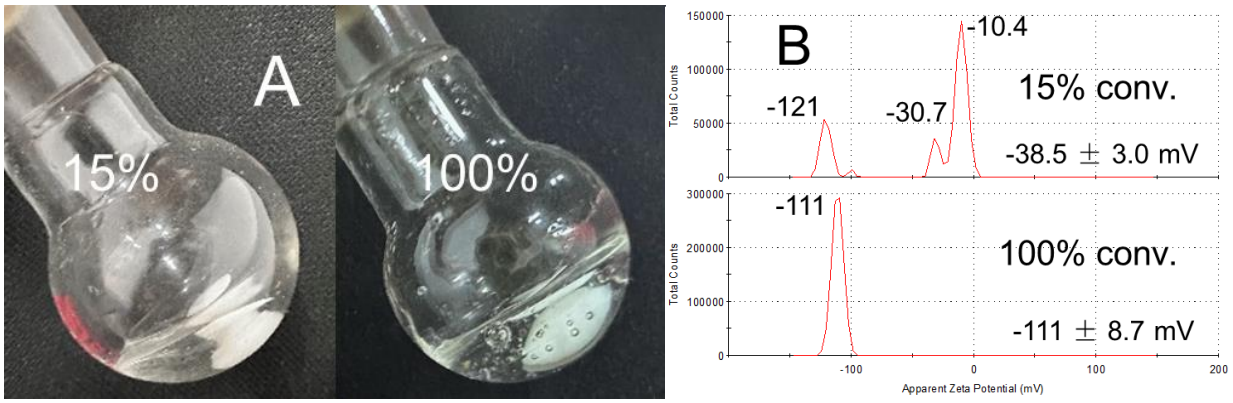

Fig. S24 (A) Digital photographs and (B) zeta potential results of the dispersions of conventional topochemical radical photopolymerization at labelled conversions.

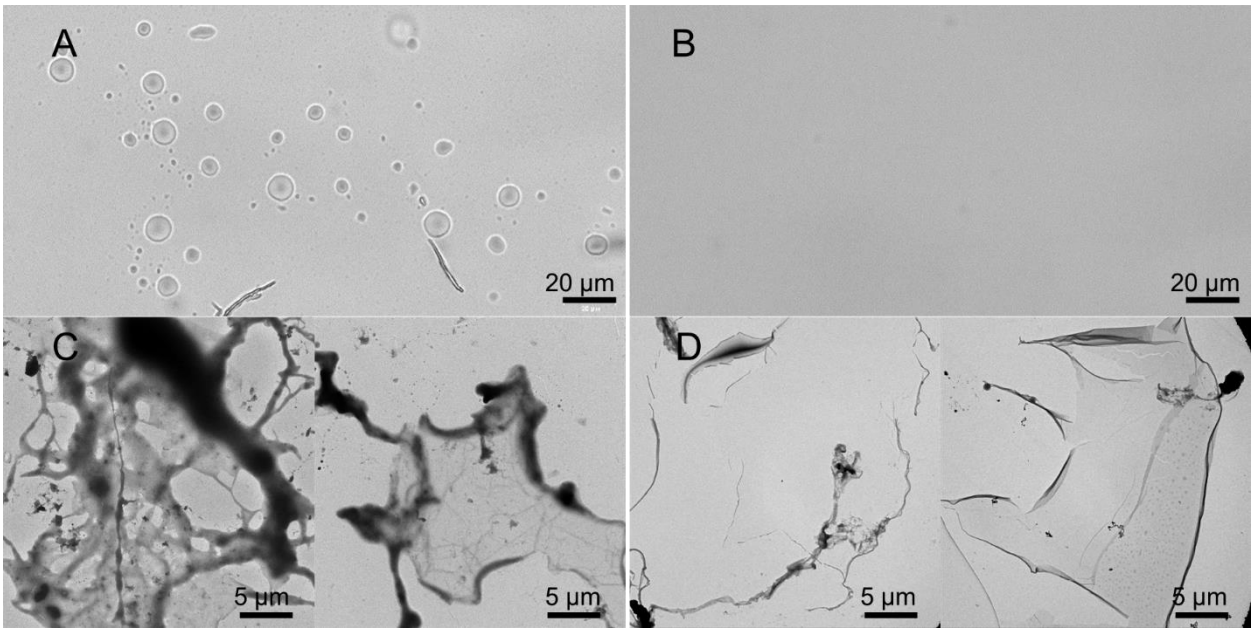

Fig. S25 Bright-field OM (top) and cryofixation TEM (bottom) images of reaction coacervates synthesized by conventional topochemical radical photopolymerization at (A, C) 15% and (B, D) 100% conversions.